Journal of Hazardous Materials 186 (2011) 738–744

Contents lists available at ScienceDirect

Journal of Hazardous Materials

journal homepage: www.elsevier.com/locate/jhazmat

Methionine–pyrene hybrid based fluorescent probe for trace level detection and estimation of Hg(II) in aqueous environmental samples: Experimental and computational studies

Arnab Banerjee, Debasis Karak, Animesh Sahana, Subarna Guha, Sisir Lohar, Debasis Das*

Department of Chemistry, The University of Burdwan, Golapbag, Burdwan, West Bengal 713 104, India

ARTICLE INFO

Article history:
Received 1 August 2010
Received in revised form
11 November 2010
Accepted 15 November 2010
Available online 23 November 2010

Keywords:
Fluorescent probe
Methionine
Pyrene
Hg^{2+}
Environmental sample
Computational studies

ABSTRACT

A new fluorescent, Hg^{2+} selective chemosensor, 4-methylsulfanyl-2-[(pyren-4-ylmethylene)-amino] butyric acid methyl ester (L, MP) was synthesized by blending methionine with pyrene. It was well characterized by different analytical techniques, *viz.* ^{1}H NMR, ^{13}C NMR, QTOF mass spectra, elemental analysis, FTIR and UV–vis spectroscopy. The reaction of this ligand with Hg^{2+} was studied by steady state and time-resolved fluorescence spectroscopy. The Hg^{2+} complexation process was confirmed by comparing FTIR, UV–vis, thermal, QTOF mass spectra and ^{1}H NMR data of the product with that of the free ligand values. The composition (Hg^{2+}:L = 1:1) of the Hg^{2+} complex in solution was evaluated by fluorescence titration method. Based on the chelation assisted fluorescence quenching, a highly sensitive spectrofluorometric method was developed for the determination of trace amounts of Hg^{2+} in water. The ligand had an excitation and emission maxima at 360 nm and 455 nm, respectively. The fluorescence life times of the ligand and its Hg^{2+} complex were 1.54 ns and 0.72 ns respectively. The binding constant of the ligand, L with Hg^{2+} was calculated using Benesi–Hildebrand equation and was found to be 7.5630×10^{4}. The linear range of the method was from 0 to 16 $\mu g\,L^{-1}$ with a detection limit of 0.056 $\mu g\,L^{-1}$ for Hg^{2+}. The quantum yields of the ligand and its Hg^{2+} complex were found to be 0.1206 and 0.0757 respectively. Both the ligand and its Hg^{2+} complex have been studied computationally (*Ab-initio*, Hartree Fock method) to get their optimized structure and other related physical parameters, including bond lengths, bond angles, dipole moments, orbital interactions etc. The binding sites of the ligand to the Hg^{2+} ion as obtained from the theoretical calculations were well supported by ^{1}H NMR titration. The interference of foreign ions was negligible. This method has been successfully applied to the determination of mercury(II) in industrial waste water.

1. Introduction

Recognition of heavy metal ions by artificial receptors has received considerable attention [1,2] due to their toxic impact on environment and living systems. Hg^{2+} ion is considered as one of the most toxic cations for environment due to its wide distribution in air, water and soil. Mercury may accumulate in the human body causing a wide variety of diseases even in a low concentration: i.e. prenatal brain damage, serious cognitive and motion disorders and minamata disease [3,4]. Hence it is desirable to develop selective and sensitive assay for Hg^{2+} ion. Several techniques for the determination of mercury ions in various samples have been reported over the past few years. They include spectrophotometry [5], atomic absorption spectrometry [6], inductively coupled plasma-atomic emission spectrometry (ICP-AES) [7] and voltammetry [8]. Although these methods offer good limits of detection and wide linear ranges, most of these techniques necessitate the use of sophisticated and costly instruments and require complicated operational procedure. Chemical sensing which combines a recognition element with an optical or electronic transduction element, serves as an efficient analytical technique for the detection of particular species [9]. Amongst various chemosensory systems, the fluorescent method is very useful due to its operational simplicity, high selectivity, sensitivity, rapidity, nondestructive methodology and direct visual perception [10]. Fluorescent chemosensors consist of a receptor and a fluorophore. The receptor is responsible for the recognition of analytes, and the fluorophore converts the recognition events into optical signals. Several fluorophore-based sensors such as dansyl, rhodamine, anthracene, naphthyl, and nile blue were reported [11]. Various type of scaffolds such as crown ether, cryptand, calixarenes, steroid, and peptides have been used as receptors for the recognition of target analytes in chemical sensors

* Corresponding author. Tel.: +91 342 2533913; fax: +91 342 2530452.
E-mail address: ddas100in@yahoo.com (D. Das).

0304-3894/$ – see front matter © 2010 Elsevier B.V. All rights reserved.
doi:10.1016/j.jhazmat.2010.11.060

[12]. In most cases, it has been observed that fluorescent chemosensors required a tedious synthetic methodology, and did not work well in aqueous solution due to their low binding affinity for the target metal ions and poor solubility in water. In recent years, considerable attention has been focused on the design of fluorescent chemo sensors for Hg^{2+} ion [13–17]. Hg^{2+} is known as a fluorescent quencher via enhancement of spin–orbit coupling [18]. Various molecular systems have been reported that monitor Hg^{2+} concentration by exploiting the mechanism of complexation-induced fluorescence quenching [19–22]. Because of its long fluorescence lifetime (up to 450 ns) [23], high fluorescence quantum yield [24] and its ability to act as a donor [25–27] as well as acceptor [28,29], pyrene has often been chosen as an ideal component in a fluorescent chemosensors for Hg(II) [30,31]. Amino acids are established metal ion receptors. Fluorescent sensors having amino acid as a metal ion receptor have hardly been found in the literature. Lee et al. reported a Fe^{3+} sensor [32] having anthracene appended amino acid (L-aspartic acid or L-glutamic acid). Sulphur containing amino acids are very effective Hg^{2+} receptors as per HSAB principle [33] Hg^{2+} sensor with sulphur bearing amino acid are not available in the literature. Herein we report, the synthesis, characterization and Hg^{2+} sensory applications of a novel fluorescent compound having pyrene–methionine hybrid structure. The method developed can selectively detect as well as estimate trace level Hg^{2+} in aqueous solution and has been successively used for the analysis of Hg^{2+} in environmental samples. The ligand and its Hg^{2+} complex have been studied theoretically by *Ab-initio* (Hartee Fock) method to have some insight about the ligand–Hg^{2+} interaction.

2. Experimental

2.1. Reagents

L-Methionine methyl ester hydrochloriode and pyrene aldehyde were purchased from Aldrich. Spectroscopy grade methanol (Merck, India) was used. Other chemicals are of analytical reagent grade and have been used without further purification except when specified. Milli-Q 18 Ω water was used throughout all the experiments. Real samples were collected from four different points of Tamla nala flowing through Durgapur industrial area (West Bengal, India), Station 1: main drain of Durgapur Chemicals Ltd. (DCL); station 2: junction of Tamla nala and main drain of DCL; station 3: upstream sample before meeting the main drain to Tamla nala; station 4: 50 m downstream from the junction of Tamla nala and main drain of DCL.

2.2. Instrumentation

A JASCO (model V-570) UV–vis spectrophotometer was used for measuring the UV–vis spectra of L and L–Hg^{2+} complex. FTIR spectra were recorded on a JASCO FTIR spectrophotometer (model: FTIR-H20). Mass spectrum was recorded in QTOF Micro YA 263 mass spectrometer in ES positive mode. Thermogravimetric analysis was performed on a Perkin Elmer TG/DTA lab system 1 (Technology by SII). ^{1}H NMR spectra were recorded using Bruker Avance 400 (400 MHz) in $CDCl_3$ using tetramethyl silane (TMS) as an internal standard. Elemental analysis was performed using Perkin Elmer CHN-Analyser with first 2000-Analysis kit. A VARIAN (Spectra AA 55) flame atomic absorption spectrophotometer (FAAS) (Australia) was used for measuring concentration of mercury by cold vapor technique. All measurements were performed using integrated absorbance (peak area). Hollow cathode lamp for Hg was operated at 4.0 mA in the wave length 324.7 nm and at a slit width of 0.5 nm. D2-back ground correction was performed in all the measurements. The steady-state fluorescence emission and excitation spectra were recorded with a Hitachi F-4500 spectrofluorometer equipped with a temperature controlled cell holder. Temperature was controlled to within ±0.1 K by circulating water from a constant temperature bath (Heto Holten, Denmark). The time-resolved fluorescence life time measurements of the free ligand and its Hg(II) complex were carried out using a time-correlated single photon counting (TCSPC) spectrometer from IBH (UK). To have an optimized structure of the ligand L, and its Hg(II) complex, *Ab-initio* calculations were performed by Hartree Fock method using 6-31G basis set and Gaussian '03 software package [34].

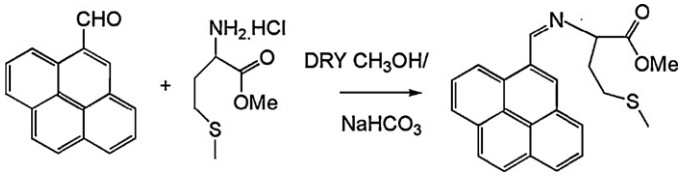

Scheme 1.

2.3. Preparation of the ligand (IUPAC, 4-methylsulfanyl-2-[(pyren-4-ylmethylene)-amino]butyric acid methyl ester) (here after, L, MP) (Scheme 1)

To a solution of 2 g (10.01 mmol) L-methionine methyl ester hydrochloriode in 50 mL dry CH_3OH was added 2.305 g (10.01 mmol, 1 equivalent) pyrene aldehyde and excess of $NaHCO_3$ (4 equivalent). The mixture was stirred over a period of 10 min followed by reflux for 6 h. On cooling, the solution was filtered through a sintered glass gooch crucible (G4) to remove unreacted $NaHCO_3$ and the filtrate was kept overnight. The orange crystalline product was isolated and dried. Yield, 65%. M.P., 85 ± 1 °C. ^{1}H NMR (400 MHz, $CDCl_3$) (Fig. S-1), δ: 2.12 (3H, s, CH_3); 2.40 (2H, m, CH_2); 2.80 (2H, m, CH_2); 3.87 (3H, s, CH_3); 4.40 (1H, t, CH); 8.47 (1H, s, –CH=N); 8.1 (d, 4H); 8.3 (s, 1H); 9.4 (d, 2H); 8.4 (m, 2H). ^{13}C NMR (200 MHz, $CDCl_3$) (Fig. S-2), δ: 172.15 (O–C=O) 163.28 (–C=N–) 133.27–122.47 (aromatic carbon), 72.30 (–CH–N), 61.44 (O–CH_3), 32.26 (N–CH_2), 30.61 (S–CH_2), 15.4 (S–CH_3), QTOF-MS ES$^+$ (Fig. S-3): $[M+H]^+$ = 376.02; elemental analysis data as calculated for $C_{23}H_{21}NO_2S$ (%): C, 73.57; H, 5.64; N, 3.73. Found (%): C, 73.27; H, 5.54; N, 3.63. FTIR (cm^{-1}): ν(CO) 1670; ν(C=N) 1503; λ_{nm} (ε, L mol^{-1} in CH_3OH at 298 K: 392 (3056), 371 (shoulder, sh) (3700), 359 (3954), 339 sh (2670), 286 (4604), 275 sh (3691), 243 (4396).

2.4. Isolation of Hg(II) complex (Scheme 2)

Methanolic solution (10 mL) of $Hg(NO_3)_2$ (181.9 mg, 0.5319 mmol) was slowly added to a methanolic solution (10 mL) of **L** (200 mg, 0.5319 mmol) and the mixture was stirred for 1 h followed by reflux for another 2 h. On slow evaporation of the solution, pale yellow flakes of the Hg^{2+} complex was isolated in 62% yield. The complex was characterized by QTOF-MS, elemental analysis, FTIR spectra and thermal studies. Elemental analysis data was calculated for $C_{23}H_{21}N_2O_5SHg$ (%): C, 43.2; H, 3.32; N, 4.39; Hg, 31.4 Found (%): C, 42.8; H, 3.37; N, 4.36; Hg, 31.8. QTOF-MS ES$^+$ (Fig. S-4) = 563.5 ($[Hg^{2+}–L+Na+H]$. FTIR (cm^{-1}): ν(CO) 1634.38; ν(C=N) 1600.63; ν(–NO_3) 1375.96; λ_{nm} (ε, L mol^{-1} in CH_3OH at 298 K: 392 (1766), 371 (shoulder, sh) (2174), 360 (2316), 339 sh (1399), 286 (3154), 275 sh (1994), 239 sh (3221), 231 (4322), 203 (2915).

2.5. Measurement procedures

Standard solutions of Hg^{2+} were obtained by serial dilution of 1.0×10^{-2} mol L^{-1} $Hg(NO_3)_2$ solution. A 10^{-4} mol L^{-1} stock solution of L was prepared by dissolving appropriate amount of L

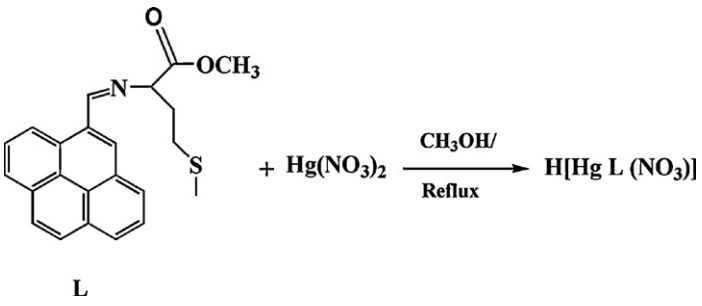

Scheme 2.

in methanol:water (2:1, v/v). The aforementioned solutions of Hg^{2+} and L were mixed in different ratios for subsequent fluorescence measurement. 1.00 cm quartz cell was used for fluorescence measurement. Anthracene was used as quantum yield standard (quantum yield is 0.27 in ethanol) [35] for measuring the quantum yields of L and L–Hg^{2+} complex.

3. Results and discussion

3.1. Spectral characteristics

Fig. 1 shows the excitation (λ = 360 nm) and emission (λ = 455 nm) spectra of L. Upon addition of Hg^{2+}, ions the fluorescence intensity at 455 nm undergoes fluorescence quenching. Pyrene monomer/excimer emission ratio strongly depends on the solvent composition [12h,36,37]. In MeOH: H_2O (2:1, v/v), mostly excimer (455 nm) emission occurs. Introduction of 50 equivalent of Hg^{2+} to a solution of L in MeOH:H_2O (2:1, v/v) results complete disappearance of excimer emission. Decrease in excimer emission intensity was attributed to the separation of the π-stacked pyrene moieties following Hg^{2+} coordination. The monomer emission was also quenched at 385 nm, attributed to the heavy atom effect. The changes in the fluorescence emission intensities of L (10^{-5} mol L^{-1}) as a function of added Hg^{2+} concentration (from 2×10^{-5} mol L^{-1} to 1×10^{-2} mol L^{-1}) were presented in Fig. 2. The plot of fluorescence intensities vs. externally added [Hg^{2+}] (Fig. 3) revealed that after a certain amount of externally added Hg^{2+}, there was no further change in the emission intensity of the system. Up to 20 times (2×10^{-4} mol L^{-1}) of the externally added [Hg^{2+}], we observed linearity. So, by making use of this linear relationship (Fig. 3), one can easily find out the concentration of any unknown Hg^{2+} species in aqueous solution. Comparison of FTIR spectra (Figs. S-5 and S-6) and UV–vis spectra (Fig. S-7) of the ligand and its Hg^{2+} complex clearly indicated complexation. On mercuration, the characteristics stretching frequencies of the ligand undergo a blue shift with a new peak at 1385 cm^{-1} indicating the presence of nitrate functionality in the Hg^{2+} complex.

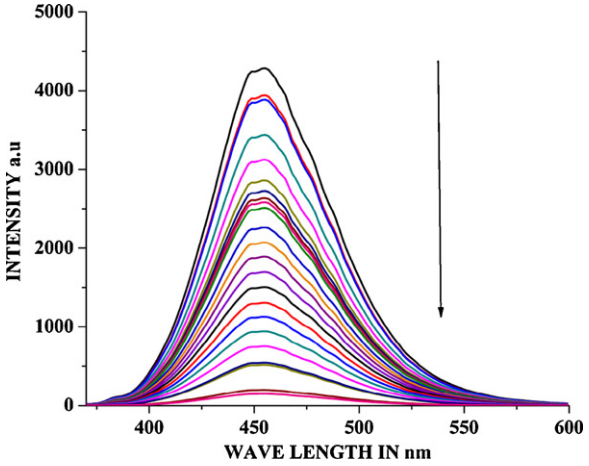

Fig. 2. Changes of the fluorescence spectra of L (10^{-5} mol L^{-1}, λ_{ex} = 360 nm) in methanol/water, 2/1 (v/v) as a function of added [Hg^{2+}].

3.2. Calculation of binding constant

Fig. 4 supported the 1:1 stoichiometry of L–Hg^{2+} complex [38]. The binding constant of the ligand L with Hg^{2+} was 7.563×10^4 (Fig. 5) as calculated using Benesi–Hildebrand equation, $I_0/(I_0 - I) = 1/A + 1/KA \times 1/[Q]$ [39] where, I_0 is the fluorescence intensity of free ligand L, I is the fluorescence intensity of the L–[Hg^{2+}] complex, Q is Hg^{2+}, A is constant and K is binding constant. Although Job's plot clearly indicated 1:1 stoichiometry of the complex but it was observed in the fluorescence titration that 50

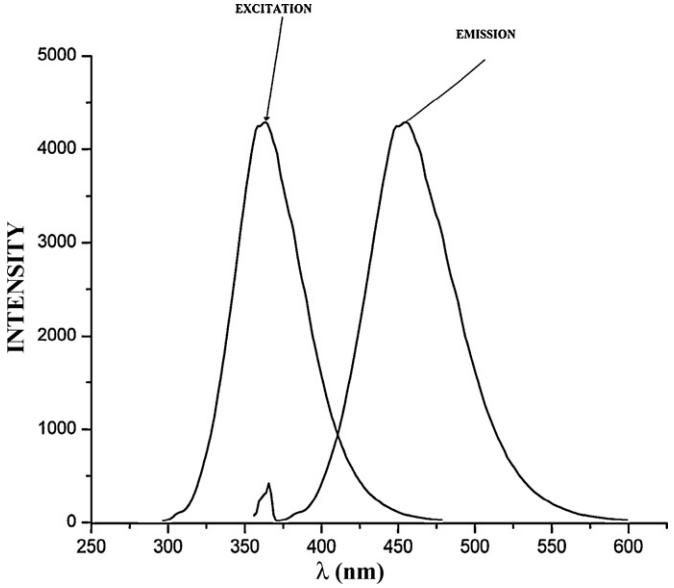

Fig. 1. Excitation (λ_{ex} = 360 nm) and emission spectra (λ_{ex} = 455 nm) of L (10^{-5} mol L^{-1}).

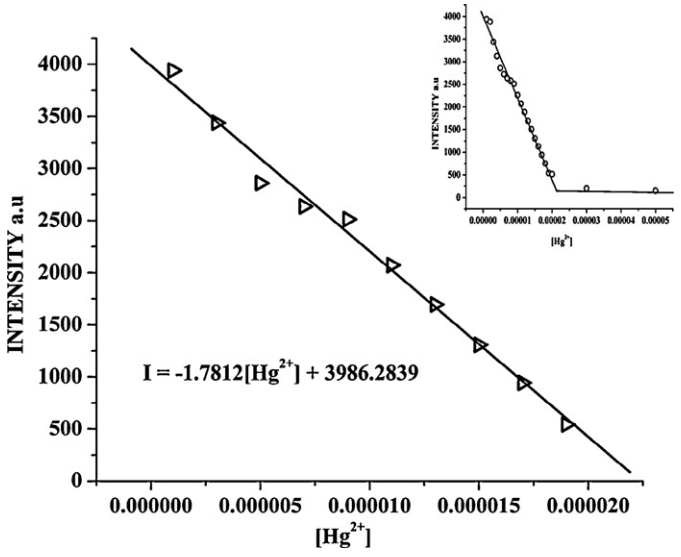

Fig. 3. Plot shows the linearity present up to [Hg^{2+}] = 20 [L]. ([L] = 10^{-5} mol L^{-1} in methanol/water, 2/1 (v/v)). Inset plot shows changes in the fluorescence intensity of the ligand as a function of added [Hg^{2+}].

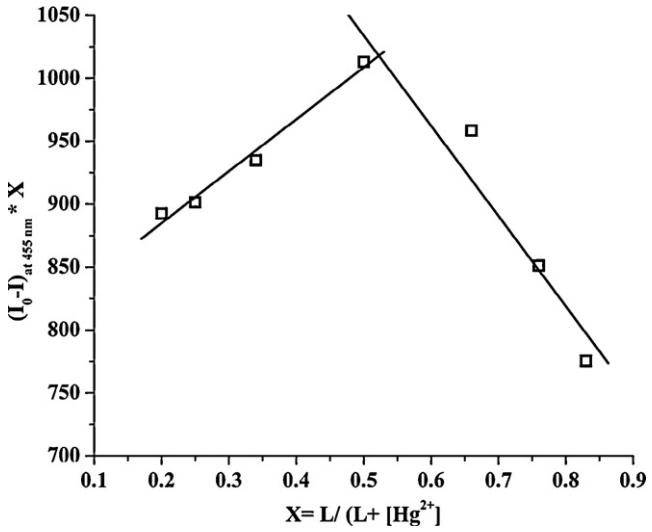

Fig. 4. Job's Plot to determine the stoichiometry of the Hg^{2+}–L complex in solution.

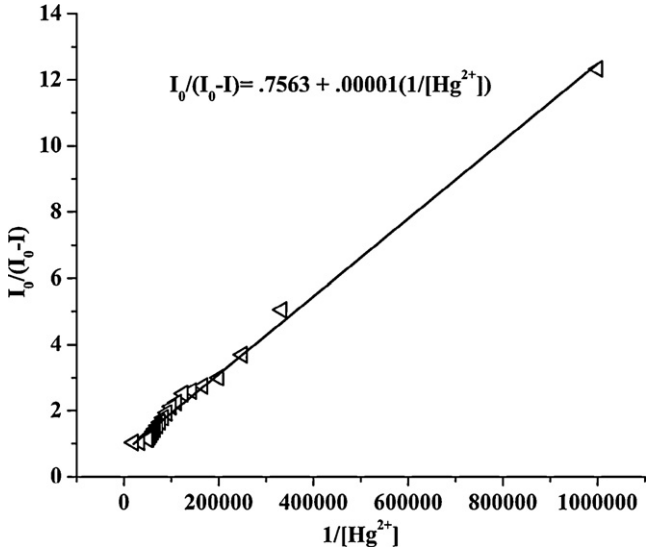

Fig. 5. Binding constant (of L with $Hg^{2+} = 7.5630 \times 10^4$) determination (Benesi–Hildebrand plot) by fluorescence method.

times [Hg^{2+}] was required to completely quench the florescence intensity of the system. This might be due to the reversibility of the reaction. Addition of large excess [Hg^{2+}] resulted the complex equilibrium to be shifted towards complex formation.

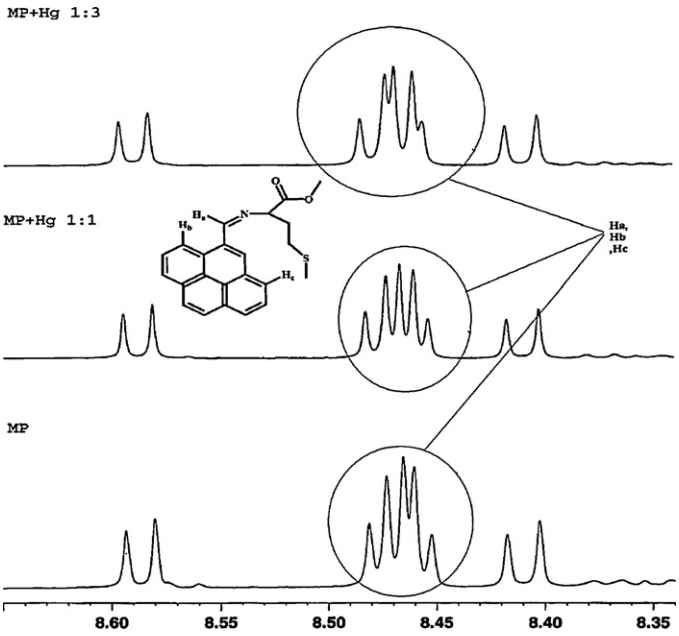

Fig. 6. ^1H NMR titration of the ligand, L, with different [Hg^{2+}] in DMSO-d_6.

3.3. NMR titration experiment

Chemical shift value of H_a (8.47 ppm) (Fig. 6) in ^1H NMR spectra of **L**, was downfield shifted on addition of Hg^{2+} indicating binding of N donor site of the Schiff base, **L** with Hg^{2+}. The minor change in the chemical shift value suggested the weak binding. The down field shift of the chemical shift value was higher in case of 1:3 (L:Hg^{2+}) mixture than 1:1 (L:Hg^{2+}) mixture, suggesting the reversibility of the complexation reaction. Moreover, on addition of Hg^{2+} to **L**, no visual change in the chemical shift value of S–CH_3 (2.12 ppm) functionality clearly indicated the reluctancy of the "S" donor site to coordinate Hg^{2+} ion (also supported by the theoretical studies).

3.4. Selectivity

The selectivity behavior was one of the most important characteristics of an ion-selective chemosensor, which was the relative optode response for the primary ion over other ions present in the solution. Thus, the influence of a number of common metal ions on the fluorescence intensity of the proposed Hg^{2+} chemosensor was investigated. In Fig. 7, effect of foreign metal ions on the fluorescence intensity of the L–Hg^{2+} system was presented. Increase in the fluorescence intensity compared to the L–Hg^{2+} system upon addition of foreign cations was designated as positive interference

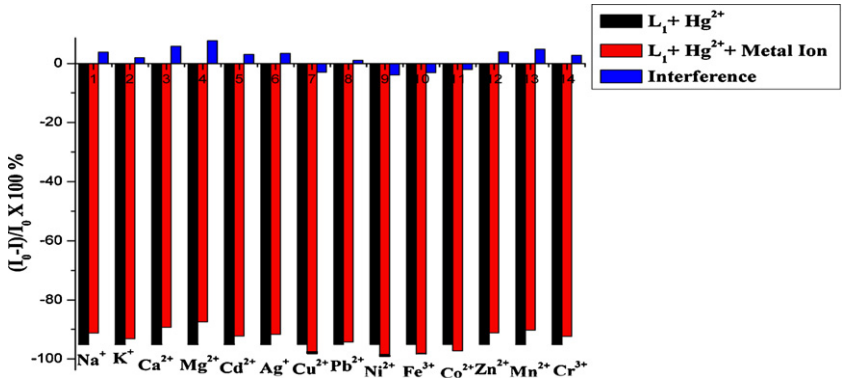

Fig. 7. Interferences from foreign cations (foreign ions are present 10 fold excess to the [Hg^{2+}].

Table 1
Radiative and the total nonradiative rate data as well as fluorescence quantum yields of L and Hg^{2+}–L complex.

	τ_F	Φ_F	k_r	k_{nr}
L (10 μM)	1.54 ns	0.1206	0.07831	0.57104
L + Hg^{2+}	0.72 ns	0.0757	0.10513	1.28375

and the reverse phenomenon was designated as negative interference. In this study, [L] = 10^{-5} mol L^{-1}, [Hg^{2+}] = 10^{-4} mol L^{-1} and the foreign metal ions were present 10 times of the [Hg^{2+}] i.e. 10^{-3} mol L^{-1}. It was observed from Fig. 5 that Na^+, K^+, Mg^{2+}, Ca^{2+}, Cd^{2+}, Ag^+, Zn^{2+}, Mn^{2+}, Cr^{3+} show insignificant positive interferences where as Cu^{2+}, Fe^{3+}, Co^{2+}, Pb^{2+}, Ni^{2+} show negligible negative interferences.

3.5. Quantum yield and florescence lifetime measurements

Fluorescence quantum yields (Φ) were estimated (Table 1) by integrating the area under the fluorescence curves using the equation,

$$\phi_{sample} = \frac{OD_{standard} \times A_{sample}}{OD_{sample} \times A_{standard}} \times \phi_{standard}$$

where *A* was the area under the fluorescence spectral curve and OD was optical density of the compound at the excitation wavelength [37].

The fluorescence life time measurement studies of the ligand in methanol/water (2:1, v/v) has been presented in Fig. 8. The effect of Hg^{2+} on the fluorescence decay behavior of L was also systematically monitored (Fig. 9) in the same solvent composition. The fluorescence life time (τ_0) of L was only 1.54 ns. In the presence of Hg^{2+} a shorter average fluorescence life time (0.72 ns) was detected. These different fluorescence life time values indicated binding of the ligand with Hg(II). Using the equation $\tau^{-1} = k_r + k_{nr}$ and $k_r = \Phi_f/\tau$ [31], the radiative rate constant k_r and the total nonradiative rate constant k_{nr} of L and L–Hg^{2+} complex were calculated and listed in Table 1. The data suggested that k_r and k_{nr} had changed almost 1.5 times and 2.25 times respectively for L and L–Hg^{2+} complex respectively. So, the factor that induced fluorescence quenching had more influence to the decrease of k_{nr} than k_r. Thus quenching was attributed to the complexation of Hg^{2+} with L, which was reconfirmed from the NMR titration experiment of L with Hg^{2+} (Fig. 6).

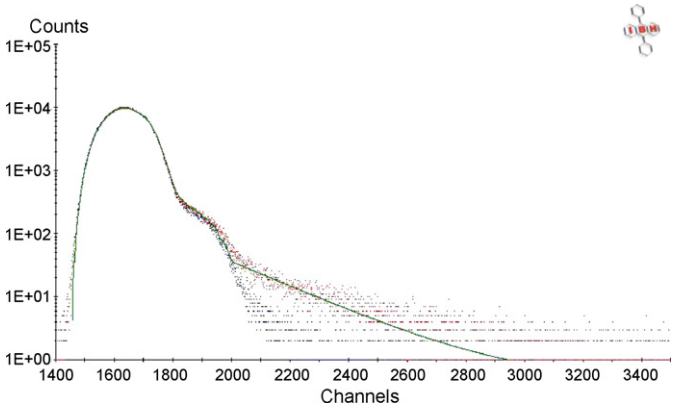

Fig. 8. Time-resolved fluorescence decay of L (10^{-5} mol L^{-1} in methanol/water, 2:1, v/v) (λ_{ex} = 360 nm).

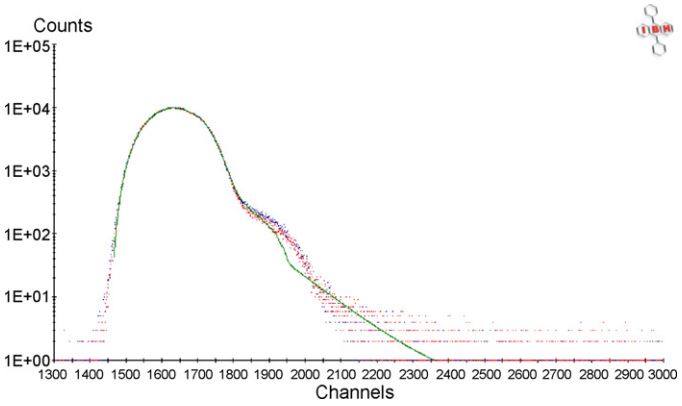

Fig. 9. Time-resolved fluorescence decay of L (10^{-5} mol L^{-1} in methanol/water, 2:1, v/v) in presence of Hg^{2+} (2×10^{-4} mol L^{-1}) (λ_{ex} = 360 nm).

3.6. Thermal studies

Stability of the ligand, L and its Hg(II) complex was studied by thermogravimetry (TGA/DTG) to prove the binding event of the ligand, L with Hg(II) ion. Results were presented in Supplementary materials (Figs. S-8 and S-9). It is clear from the graphs that thermal stability of the Hg(II) complex (up to 150 °C) is more than the free ligand (up to 100 °C). Mass loss calculation from the TGA curve of the Hg^{2+} complex at 150 °C (weight loss of 11%) suggested the loss of nitrate moiety.

3.7. Computational studies

Figs. 10 and 11 present the stereoscopic view of the optimized structures of the ligand, L and its Hg(II) complex. All the bond lengths and bond angles of both the structures are available as Supplementary materials (Table S-1). In the nitrate bound Hg^{2+} complex, the bond lengths of Hg–O and Hg–N (imine) were 2.24 Å and 2.26 Å respectively. The Hg–S bond length was 2.72 Å which is much higher than a single bond and excluded the possibility of "S" coordination to the Hg^{2+} which was also reflected in the NMR titration where no visual change in the chemical shift value of S–CH_3 (2.12 ppm) functionality was observed. Highest occupied molecular orbitals (HOMOs) of the ligand L and L–Hg^{2+} complex were presented in Figs. 12 and 13 respectively. Whereas lowest unoccupied molecular orbitals (LUMOs) of the ligand L and L–Hg^{2+} complex were presented in Figs. 14 and 15 respectively. The distinctive nature of their HOMOs and LUMOs also suggested the binding

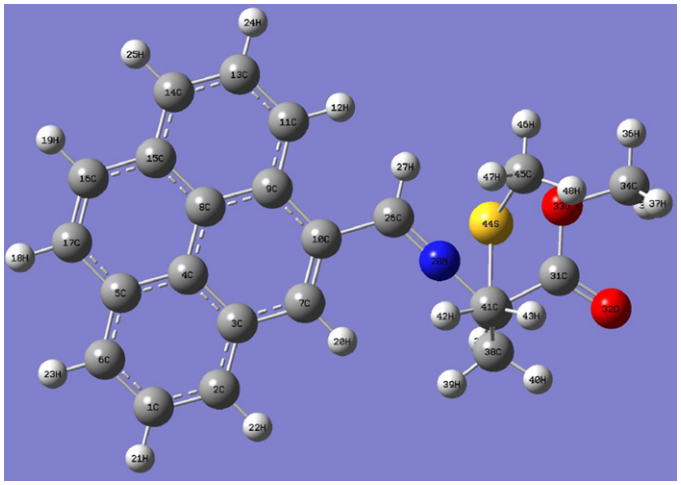

Fig. 10. Stereoscopic view of the ligand obtained from *Ab-initio* studies (Hartree Fock method).

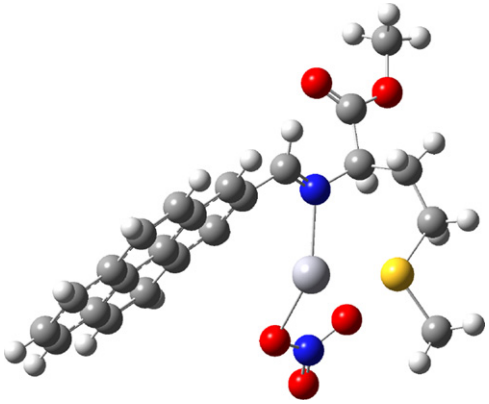

Fig. 11. Stereoscopic view of the Hg^{2+}–L complex obtained from *Ab-initio* studies (Hartree Fock method).

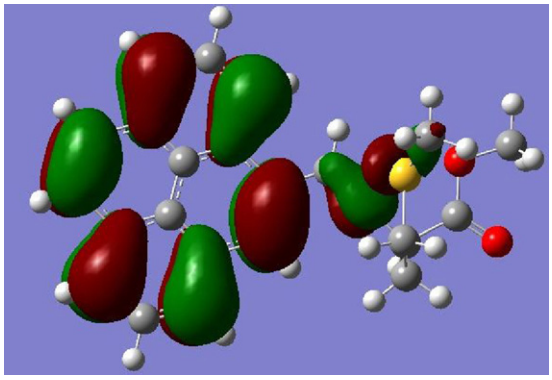

Fig. 12. Highest occupied molecular orbital of ligand, L.

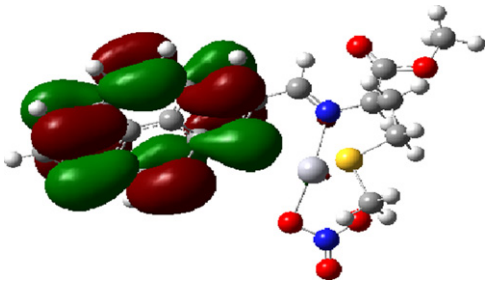

Fig. 13. Highest occupied molecular orbital of Hg^{2+}–L complex.

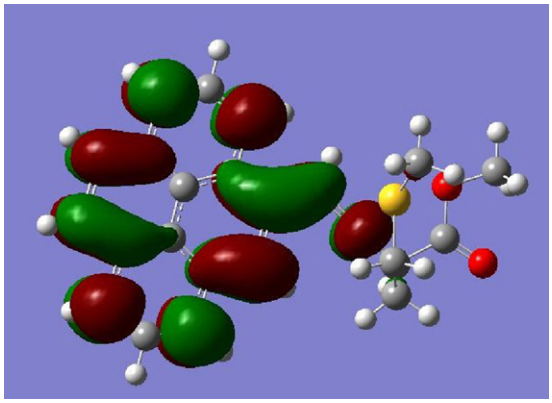

Fig. 14. Lowest unoccupied molecular orbital of ligand, L.

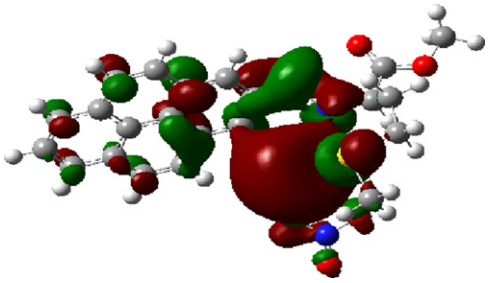

Fig. 15. Lowest unoccupied molecular orbital of L + Hg^{2+}.

Table 2
Analysis of certified reference materials and real (industrial waste water) samples.

Sample	Hg^{2+} found[a] ($\mu g\,g^{-1}$) using the present method	Hg^{2+} found ($\mu g\,g^{-1}$) using the reference method[c]
Industrial waste water (station 1)	140.2 ± 0.6	140.7 ± 0.4
Industrial waste water (station 2)	180.2 ± 0.8	179.8 ± 0.2
Industrial waste water (station 3)	165.2 ± 0.4	165.6 ± 0.3
Industrial waste water (station 4)	225.9 ± 0.3	226.4 ± 0.6
NIES certified sample[b]	1.11 ± 0.7	1.14 ± 0.2

[a] Average was calculated with $N = 3$.
[b] NIES certified value: 1.2 ± 0.2.
[c] Ref. [28].

ability of the ligand to Hg^{2+}. The dipole moment values of the ligand and its Hg^{2+} complex, as found from the theoretical studies were 2.0878 Debye and 9.3839 Debye respectively, which indicated greater charge separation in the Hg^{2+} complex compared to the free ligand, plausibly due to the transfer of electrons from the ligand to the Hg^{2+} ion. Different parameters like, bond moments, dipole moments, quadruple moments along with optimized energies of the ligand L and L+ Hg^{2+} complex are presented in Supplementary materials.

3.8. Application

The validity of this newly developed method was checked by analyzing certified reference materials. Some real samples (industrial waste water) were analyzed and compared with a reference method [40]. The results were presented in Table 2. The industrial waste water samples were collected from Damodar river (Durgapur-Raniganj Industrial belt, West Bengal, India) and filtered through 0.45 μm Milipore membrane filter followed by its analysis with the proposed chemosensor. The close proximity of the results of analysis of the certified reference materials by the present method clearly indicated its acceptability for the determination of Hg^{2+} in real samples.

4. Conclusion

The well characterized new ligand (L, MP) was very selective for trace level detection and estimation of inorganic Hg^{2+} from aqueous solution. The binding constant of the ligand with Hg^{2+} was fairly high. ^1H NMR titration and time resolved fluorescence life time measurements also proved the binding between the ligand, L with Hg^{2+}. UV–vis and FTIR spectra of the ligand and Hg^{2+} complex clearly indicated the complexation process. Composition of the L–Hg^{2+} complex was confirmed by the QTOF-MS ES^+ mass spectra in solid state and by the Job's method in solution. Finally, computational studies were performed to have a stereoscopic view of the structures of the ligand and its Hg^{2+} complex which also provided their different structural information. The analysis of certified reference materials and real samples were carried out by this new method.

Acknowledgements

The authors are grateful to IUC-DAE, Kolkata Centre and DST (Govt. of W.B.) for funding. Animesh Sahana, Sisir Lohar and Debasis Karak are grateful to CSIR and UGC, New Delhi for providing fellowship to them.

Appendix A. Supplementary data

Supplementary data associated with this article can be found, in the online version, at doi:10.1016/j.jhazmat.2010.11.060.

References

[1] A.P. de Silva, D.B. Fox, A.J.M. Huxley, T.S. Moody, Combining luminescence, coordination and electron transfer for signaling purposes, Chem. Rev. 205 (2000) 41–57.
[2] A.P. de Silva, H.Q.N. Gunaratne, T. Gunnlaugsson, A.J.M. Huxley, C.P. McCoy, J.T. Rademacher, T.E. Rice, Signaling recognition events with fluorescent sensors and switches, Chem. Rev. 97 (1997) 1515–1566.
[3] P. Grandjean, P. Weihe, R.F. White, F. Debes, Cognitive performance of children prenatally exposed to "Safe" levels of methylmercury, Environ. Res. 77 (1998) 165–172.
[4] M. Harada, Minamata disease: methylmercury poisoning in Japan caused by environmental pollution, Crit. Rev. Toxicol. 25 (1995) 1–24.
[5] M.S. Hosseini, H. Hashemi-Moghaddam, Sensitized extraction spectrophotometric determination of Hg(II) with dithizone after its flotation as ion-associate using iodide and ferroin, Talanta 67 (2005) 555–559.
[6] J.L. Manzoori, M.H. Sorouraddin, A.M.H. Shabani, Determination of mercury by cold vapour atomic absorption spectrometry after preconcentration with dithizone immobilized on surfactant-coated alumina, J. Anal. Atom. Spectrom. 13 (1998) 305–308.
[7] A.N. Anthemidis, G.A. Zachariadis, C.E. Michos, J.A. Stratis, Time-based on-line preconcentration cold vapour generation procedure for ultra-trace mercury determination with inductively coupled plasma atomic emission spectrometry, Anal. Bioanal. Chem. 379 (2004) 764–769.
[8] H. Zejli, P. Sharrock, J.L.H.H. de Cisneros, I. Naranjo-Rodriguez, K.R. Temsamani, Voltammetric determination of trace mercury at a sonogel–carbon electrode modified with poly-3-methylthiophene, Talanta 68 (2005) 79–85.
[9] J.P. Desvergne, A.W. Czarnik, Chemosensors of Ion and Molecule Recognition, NATO ASI Series, Kluwer Academic, Dordrecht, 1997.
[10] A.W. Czarnik, Fluorescent Chemosensors for Ion and Molecule Recognition ACS Symposium Series, vol. 538, American Chemical Society, Washington, 1992.
[11] (a) S. Deo, A.G. Goldwin, A selective, ratiometric fluorescent sensor for Pb^{2+}, J. Am. Chem. Soc. 122 (2000) 174–175;
(b) X. Che, S.W. Nam, Y. Kim, S.J. Kim, S. Park, J. Yoon, Hg^{2+} selective fluorescent and colorimetric sensor: its crystal structure and application to bioimaging, Org. Lett. 10 (2008) 5235–5238;
(c) Z.C. Xu, S.K Kim, K.H. Lee, J.Y. Yoon, A highly selective fluorescent chemosensor for dihydrogen phosphate via unique excimer formation and PET mechanism, Tetrahedron Lett. 48 (2007) 3797–3800;
(d) M.H. Lee, S.W. Lee, S.H. Kim, C. Kang, J.S. Kim, Nanomolar Hg(II) detection using nile blue chemodosimeter in biological media, Org. Lett. 11 (2009) 2101–2104;
(e) K.J. Parker, S. Kumar, D.A. Pearce, A.J. Sutherland, Design, synthesis and evaluation of a fluorescent peptidyl sensor for the selective recognition of arsenite, Tetrahedron Lett. 46 (2005) 7043–7045.
[12] (a) B.P. Joshi, W.M. Cho, J. Kim, J. Yoon, K.H. Lee, Design, synthesis, and evaluation of peptidyl fluorescent probe for Zn^{2+} in aqueous solution, Bioorg. Med. Chem. Lett. 17 (2007) 6425–6429;
(b) B.P. Joshi, J. Park, W.I. Lee, K.H. Lee, Ratiometric and turn-on monitoring for heavy and transition metal ions in aqueous solution with a fluorescent peptide sensor, Talanta 78 (2009) 903–909;
(c) J.S. Kim, D.T. Quang, Calixarene-derived fluorescent probes, Chem. Rev. 107 (2007) 3780–3799;
(d) Y. Zhao, Z. Zhong, Detection of Hg^{2+} in aqueous solutions with a foldamer-based fluorescent sensor modulated by surfactant micelles, Org. Lett. 8 (2006) 4715–4717;
(e) J.F. Callan, A.P. de Silva, D.C. Magri, Luminescent sensors and switches in the early 21st century, Tetrahedron 61 (2005) 8551–8558;
(f) T.W. Bell, N.M. Hext, Supramolecular optical chemosensors for organic analytes, Chem. Soc. Rev. 33 (2004) 589–598;
(g) K. Rurack, U. Resch-Genger, Rigidization, preorientation and electronic decoupling – the 'magic triangle for the design of highly efficient fluorescent sensors and switches, Chem. Soc. Rev. 31 (2002) 116–127;
(h) A.P. de Silva, H.Q.N. Gunaratne, T. Gunnlaugsson, J.M.H. Allen, C.P. McCoy, J.T. Rademacher, T.E. Rice, Signaling recognition events with fluorescent sensors and switches, Chem. Rev. 97 (1997) 1515–1566.
[13] (a) M. Kumar, A. Dhir, V. Bhalla, R. Sharma, R.K. Puri, R.K. Mahajan, Highly effective chemosensor for mercury ions based on bispyrenyl derivative, Analyst 135 (2010) 1600–1605;
(b) Y. Zhou, C.-Y. Zhu, X.-S. Gao, X.-Y. You, C. Yao, Hg^{2+} selective ratiometric and "off-on" chemosensor based on the azadiene–pyrene derivative, Org. Lett. 12 (2010) 2566–2569;
(c) R. Guliyev, A. Coskun, E.U. Akkaya, Design strategies for ratiometric chemosensors: modulation of excitation energy transfer at the energy donor site, J. Am. Chem. Soc. 131 (2009) 9007–9013.
[14] E.M. Nolan, S.J. Lippard, Tools and tactics for the optical detection of mercuric ion, Chem. Rev. 108 (2008) 3443–3480.
[15] Y.-K. Yang, K.-J. Yook, J. Tae, A rhodamine-based fluorescent and colorimetric chemodosimeter for the rapid detection of Hg^{2+} ions in aqueous media, J. Am. Chem. Soc. 127 (2005) 16760–16761.
[16] X. Guo, X. Qian, L. Jia, A highly selective and sensitive fluorescent chemosensor for Hg^{2+} in neutral buffer aqueous solution, J. Am. Chem. Soc. 126 (2004) 2272–2273.
[17] E.M. Nolan, S.J. Lippard, A "turn-on" fluorescent sensor for the selective detection of mercuric ion in aqueous media, J. Am. Chem. Soc. 125 (2003) 14270–14271.
[18] D.S. McClure, Spin–orbit interaction in aromatic molecules, J Chem. Phys. 20 (1952) 682.
[19] A.B. Descalzo, R.M. Mañez, R. Radeglia, K. Rurack, J. Soto, Coupling selectivity with sensitivity in an integrated chemosensor framework: design of a Hg^{2+}-responsive probe, operating above 500 nm, J. Am. Chem. Soc. 125 (2003) 3418–3419.
[20] Y. Zhao, Z. Zhong, Tuning the sensitivity of a foldamer-based mercury sensor by its folding energy, J. Am. Chem. Soc. 128 (2006) 9988–9989.
[21] S.Y. Moon, N.R. Cha, Y.H. Kim, S.-K. Chang, New Hg^{2+}-selective chromo- and fluoroionophore based upon 8-hydroxyquinoline, J. Org. Chem. 69 (2004) 181–183.
[22] S.Y. Moon, N.J. Youn, S.M. Park, S.-K. Chang, Diametrically disubstituted cyclam derivative having Hg^{2+}-selective fluoroionophoric behaviors, J. Org. Chem. 70 (2005) 2394–2397.
[23] J.B. Birks, D.J. Dyson, I.H. Munro, The relations between the fluorescence and absorption properties of organic molecules, Proc. Roy. Soc. 275 (1963) 135–148.
[24] S. Leroy-Lhez, F. Fages, Synthesis and photophysical properties of a highly fluorescent ditopic ligand based on 1,6-bis(ethynyl)pyrene as central aromatic core, Eur. J. Org. Chem. 13 (2005) 2684–2688.
[25] T. Fiebig, K. Stock, S. Lochbrunner, E. Riedle, Femtosecond charge transfer dynamics in artificial donor/acceptor systems: switching from adiabatic to nonadiabatic regimes by small structural changes, Chem. Phys. Lett. 345 (2001) 81–88.
[26] R.D. Fossum, M.A. Fox, Dual exciplex formation and photoinduced electron transfer in pyrene end-labeled polynorbornenes, J. Phys. Chem. B 101 (1997) 6384–6393.
[27] T.L. Netzel, K. Nafisi, J. Headrick, B.E. Eaton, Direct observation of photoinduced electron transfer in pyrene-labeled du nucleosides and evidence for protonated 2′-deoxyuridine anion, dU(H), as a primary electron transfer product, J. Phys. Chem. 99 (1995) 17948–17955.
[28] E. Austin, M. Gouterman, Porphyrins. XXXVII. Absorption and emission of weak complexes with acids, bases, and salts, Bioinorg. Chem. 9 (1978) 281–298.
[29] G.H. Zhang, J.K. Thomas, A. Eremenko, T. Kikteva, F. Wilkinson, Photoinduced chargetransfer reaction between pyrene and N,N′-dimethylaniline on silica gel surfaces, J. Phys. Chem. B 101 (1997) 8569–8577.
[30] S.Y. Moon, N.J. Youn, S.M. Park, S.K. Chang, Diametrically disubstituted cyclam derivative having Hg^{2+}-selective fluoroionophoric behaviors, J. Org. Chem. 70 (2005) 2394–2397.
[31] S.M. Park, M.H. Kim, J.I. Choe, K.T. No, S.-K. Chang, Cyclams bearing diametrically disubstituted pyrenes as Cu^{2+}- and Hg^{2+}-selective fluoroionophores, J. Org. Chem. 72 (2007) 3550–3553.
[32] C.R. Lohani, J.-M. Kim, K.-H. Lee, Facile synthesis of anthracene-appended amino acids as highly selective and sensitive fluorescent Fe^{3+} ion sensors, Bioorg. Med. Chem. Lett. 19 (2009) 6069–6073.
[33] Y.K. Sze, A.R. Davis, G.A. Neville, Raman and infrared studies of complexes of mercury(II) with cysteine, cysteine methyl ester and methionine, Inorg. Chem. 14 (1975) 1969–1974.
[34] W.H. Melhuish, Quantum efficiencies of fluorescence of organic substances: effect of solvent and concentration of the fluorescent solute, J. Phys. Chem. 65 (1961) 229–235.
[35] Gaussian 03, Rev.C.02, Gaussian Inc., Wallingford CT, 2004.
[36] A. Wiessner, W. Kuhnle, T. Fiebig, H. Staerk, Intramolecular charge transfer (ICT) and solvation of a rigidly linked pyrene/N-methylindolino derivative and related compounds in linear alcohols, J. Phys. Chem. A 101 (1997) 350–359.
[37] (a) N.J. Turro, Modern Molecular Photochemistry, Benjamin Cummings, Menlo Park, 1978.
[38] K.A. Connors, Binding Constants, Wiley, New York, 1987.
[39] H.A. Benesi, J.H. Hildebrand, A spectrophotometric investigation of the interaction of iodine with aromatic hydrocarbons, J. Am. Chem. Soc. 71 (1949) 2703–2707.
[40] E.M. Soliman, M.B. Saleh, S.A. Ahmed, New solid phase extractors for selective separation and preconcentration of mercury(II) based on silica gel immobilized aliphatic amines 2-thiophenecarboxaldehyde Schiff's bases, Anal. Chim. Acta 523 (2004) 133–140.